Spring 2018

Multi-Parented End-Effectors in Optimization-Based Prediction of Posture and Anthropometry

Anna Seydel
University of Iowa

MULTI-PARENTED END-EFFECTORS IN OPTIMIZATION-BASED PREDICTION OF POSTURE AND ANTHROPOMETRY

by

Anna Seydel

A thesis submitted in partial fulfillment of the requirements
for graduation with Honors in the Biomedical Engineering

_____

Karim Abdel-Malek
Thesis Mentor

Spring 2018

All requirements for graduation with Honors in the
Biomedical Engineering have been completed.

_____

David Wilder
Biomedical Engineering Honors Advisor

MULTI-PARENTED END-EFFECTORS IN OPTIMIZATION-BASED PREDICTION OF POSTURE AND ANTHROPOMETRY

University of Iowa
Department of Biomedical Engineering
Submitted By: Anna Seydel

ABSTRACT

Improving motion capture processing onto a virtual model is an important research area. Although there has been significant research in this field, little work has been done to determine posture and anthropometry simultaneously with the intent of visualizing the data on virtual models. Many existing techniques are less accurate when applying processed data to a virtual model for biomechanical analysis. This paper presents a novel approach that estimates posture and anthropometry using optimization-based posture prediction to determine joint angles and link-lengths of a virtual model. By including anthropometric design variables, this approach introduces flexible handling of innate variance in subject-model measurements without need for pre- or post-processing. This produces a more realistic motion and exhibits anthropometric measurements closer to those of the original subject, resulting in a new level of biomechanical accuracy that allows for analysis of a processed motion with a higher degree of confidence.

1 INTRODUCTION

The increasing demand for accurate evaluation of biomechanical factors related to human motion on a virtual model calls for improvement in the processing and subsequent visualization of motion capture data. Specifically, there is a growing need to process motion capture data for highly articulated three-dimensional human models capable of replicating complex human motion. Use of motion capture technology has primarily been in the entertainment and gaming industry for visualizing motion or enhancing the animated motion of cinematic characters. More recently, however, motion capture technology has gained traction in the field of biomechanics in such applications as injury prevention and gait analysis.

At the Center for Computer Aided Design (CCAD), motion capture plays a significant role in several projects. A specific sector of CCAD, known as Virtual Soldier Research (VSR), utilizes motion capture technology as a basis for visualizing human motion. While its name stems from its initial Navy-funded research, VSR is involved in non-military-based projects, including studies in biomechanics such as injury prediction software. A majority of these biomechanical studies rely on a mathematical description of movement, which provides a basis for the quantitative evaluation of human performance. The processing of the retrieved motion data onto a virtual model makes it possible to analyze attributes that are difficult to observe on real-world human subjects [1]. However, use in this capacity requires improved accuracy of methods for processing the raw data and translating it to biomechanically relevant parameters.

Current techniques are unable to adequately account for the variance in anthropometric measurements between the original subject from which the motion was captured and the high-fidelity virtual model on which the data is processed. Consequently, it is difficult to visualize human motion on a high-fidelity model and perform accurate biomechanical analysis using the processed data. As discussed by Bonin et al., one method to overcome this obstacle is to utilize anthropometric databases in the generation of the virtual model. An advantage of this method includes the increased similarity between the anthropometric measurements of the original subject and the virtual model. Adversely, there are certain obstacles, such as dealing with data for which the dimensions of the original subject are not available. Furthermore, it also requires reconstruction of the virtual model from three-dimensional scans, necessitating further tools and time [2].

Generally, a virtual model is categorized as either an anthropometric model, used for analysis of human dimension and body shape, or a biomechanical model, used for analysis and simulation of motion [3]. Given the need for biomechanical analysis and the extreme variability of human body parameters, it is necessary to provide a flexible method that considers both anthropometric and kinematic factors— specifically, a method that is capable of handling the diverse anthropometric measurements of the human population, thus providing the means to analyze processed human motion with a higher degree of confidence. This paper presents a new approach to motion processing that estimates both posture and anthropometry simultaneously using optimization-based

techniques. By including anthropometric design variables, this approach introduces a flexible method for handling innate variance in subject-model measurements without the need for pre/post-processing or virtual model generation. Using this optimization-based approach, the need for an anthropometric human model and a biomechanical human model can be satisfied with a single representation. This produces a more realistic motion and exhibits anthropometric measurements closer to those of the original subject, resulting in a higher level of biomechanical accuracy.

2 BACKGROUND

2.1 Kinematic Human Model

The human body can be mathematically represented using a series of rigid links connected at vertices that are representative of joints. Each joint has between one and three degrees-of-freedom (DOF), dependent on the ability of the joint to rotate about the x-, y-, and z-axis [4]. The model in this study (Santos™) is a 55-DOF articulated kinematic chain as shown in
Fig. 1. 55-DOF kinematic human model used during posture prediction and motion simulation..

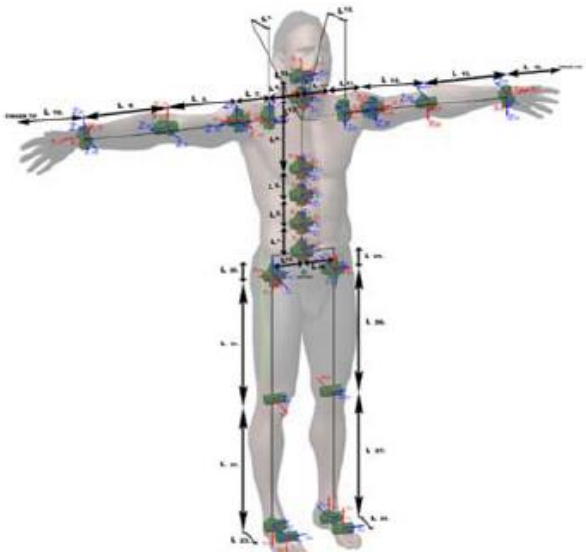

Fig. 1. 55-DOF kinematic human model used during posture prediction and motion simulation.

The location and orientation of each joint and link depicted in the model exhibited in Fig. 1 follows the Denavit-Hartenberg (DH) convention [5]. Although the DH method is traditionally used in the robotics field, it has been used effectively for modeling human biomechanics in optimization-based posture prediction [14]. Four parameters of the DH method provide a convenient and systematic way of representing joint translation. A local coordinate frame is associated with each DOF, and is used to represent the transformation from one DOF frame to the next in the kinematic chain. DH convention imposes restrictions on the local coordinate system at each DOF, such that the $(i-1)^{th}$

z-axis represents the axis motion for the (i)th DOF. The position and orientation of this frame with respect to frame i – 1 can be found with the four DH parameters, described by Farrell (2005) as follows:

I. Θ_i – Angle between the (i - 1)th and ith x-axis about the (i - 1)th z-axis
II. d_i – Distance from the (i - 1)th to the ith x-axis along the (i - 1)th z-axis
III. α_i – Angle between the (i - 1)th and ith z-axis about the ith x-axis
IV. a_i – Distance from the (i - 1)th to the ith x-axis along the ith x-axis

Through the use of these parameters, the global position vector $\boldsymbol{x(q)}$ of any local position $\boldsymbol{x_n}$ given relative to the n^{th} frame is given by:

$$\boldsymbol{x}(\boldsymbol{q}) = \left(\prod_{i=1}^{n} {}^{i-1}\boldsymbol{T}_i \right) \boldsymbol{x_n} \tag{2.1}$$

$${}^{i-1}\boldsymbol{T}_i = \begin{bmatrix} \cos\theta_i & -\cos\alpha_i \sin\theta_i & \sin\alpha_i \sin\theta_i & \alpha_i \cos\theta_i \\ \sin\theta_i & \cos\alpha_i \cos\theta_i & -\sin\alpha_i \cos\theta_i & \alpha_i \sin\theta_i \\ 0 & \sin\alpha_i & \cos\alpha_i & d_i \\ 0 & 0 & 0 & 1 \end{bmatrix} \tag{2.2}$$

Eq. 2.1 and 2.2 can be used to calculate the global position of two separate entities referred to in this paper. The first of these is the local target positions given by the motion capture data, and the second is the end-effector markers placed on the virtual model. Both of these calculations can be used in the optimization-based posture prediction problem, which allows for visualization of motion on the highly-articulated, kinematic human model.

2.2 Optimization-Based Posture Prediction

The goal of posture prediction is to determine a conformation of kinematic joint angles that allows the virtual model body to satisfy a particular requirement; for instance, touch a particular point in a workspace with a specified fingertip. Posture problems are often redundant with many possible solutions. To distinguish between solutions, the optimization-based approach minimizes an objective function. Objective functions are mathematically representative of the driving factors of human posture, such as the desire to maintain neutral posture [8], reduce joint discomfort [9], or maintain visual contact with a given target [10]. The formulation is given as [11]:

$$\begin{gathered} \text{Find: } \boldsymbol{q} \in R^{DOF} \\ \text{Minimize: } f(\boldsymbol{x}(\boldsymbol{q})) \textit{ (Discomfort, Effort, etc.)} \\ \text{Subject to: } \left\| \boldsymbol{x}(\boldsymbol{q})^{end-effector} - \boldsymbol{x}^{target\ point} \right\|^2 \leq \varepsilon \\ \text{and} \quad q_i{}^L \leq q_i \leq q_i{}^H;\ i = 1, 2, \ldots, DOF \end{gathered} \tag{2.3}$$

In the above equation, $\boldsymbol{q}$ is a vector of joint angles, $\boldsymbol{x}$ is the position of an end-effector (i.e. marker on the virtual model), ε is a small positive number that approximates zero, and DOF is the total number of degrees of freedom. The function $f(\boldsymbol{x}(\boldsymbol{q}))$ can be one of many objective functions, as discussed previously. The primary constraint, called the distance constraint, requires the end-effector(s) to contact a specified target point(s). Additionally, ${q_i}^U$ represents the upper limit, and ${q_i}^L$ represents the lower limit of a joint *i* as derived from kinematic data. In addition to these basic constraints, many others can be incorporated as boundary conditions to fully describe the present virtual environment.

2.3 Motion Capture Processing

Most motion capture systems provide the three-dimensional Cartesian position of each target marker placed on the subject at each frame of the motion, allowing the positions of the target markers to be represented in a virtual environment at each frame [12]. For the purposes of this paper, processing such motion capture data refers to using these target marker positions as input to replicate the motion on a virtual model, where the motion is ultimately described by a vector of joint angles that changes over time. Markers of this type will be referred to as target markers, as they are the end positional target of a corresponding end-effector.

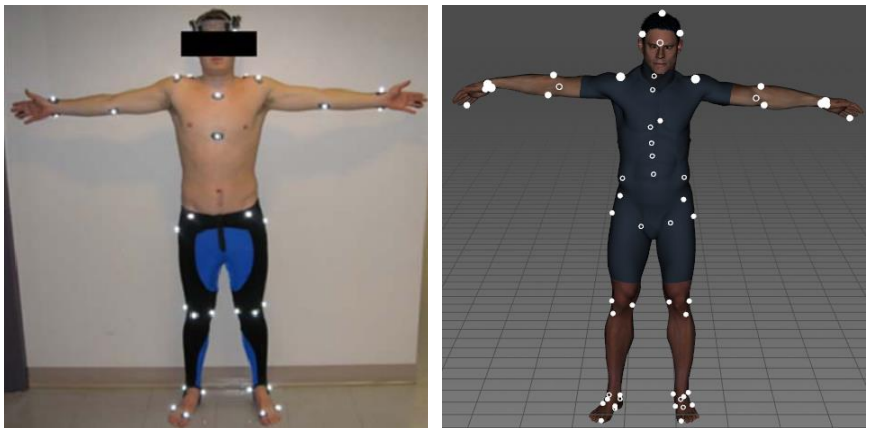

(a) (b)

Fig. 2. Mapping Target markers on the human subject onto the virtual model: (a) target markers [13] (b) virtual end-effectors.

A mapping protocol is used to place end-effectors on the virtual model (**Error! Not a valid bookmark self-reference.**b), which correspond to the anatomical locations of the target markers as they were placed on the subject (**Error! Not a valid bookmark self-reference.**a). The protocol defines each of these end-effectors relative to a parent joint on the high-fidelity human model and maps each marker onto the model relative to a global coordinate system in three-dimensional space [13].

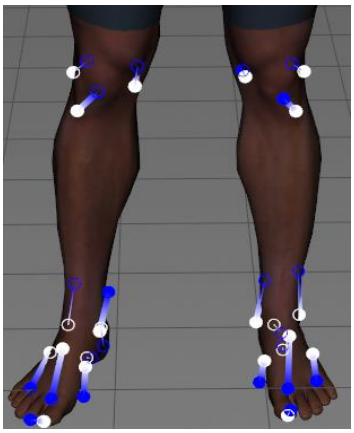

Fig. 3. Close-up of distances between target markers (white) and end-effectors (blue) on virtual model.

In Fig. 3, the end-effectors are depicted in blue. To process an individual frame of the motion capture data, a distance objective is created for each end-effector to minimize the distance to its mapped target obtained from the motion capture data. To replicate an entire motion, posture prediction is executed over all frames to determine joint angles using the formulation defined in Eq. 2.3.

Because this formulation creates one distance objective for each of the end-effectors, a p-norm multi-objective optimization (MOO) representative of overall positional error is defined as [14]:

$$\boldsymbol{f}(\boldsymbol{x}(\boldsymbol{q})) = \left[\sum_{\boldsymbol{i=1}}^{\boldsymbol{n}} \left(\boldsymbol{w_i} \frac{\|\boldsymbol{x_i}(\boldsymbol{q}) - \boldsymbol{t_i}\|^2}{\boldsymbol{d_{max}}}\right)^{\boldsymbol{p}}\right]^{\frac{1}{\boldsymbol{p}}} \tag{2.4}$$

In the above equation, $\boldsymbol{p} = \boldsymbol{2}$, and $\boldsymbol{x_i}(\boldsymbol{q})$ refers to the position of each end-effector, which is dependent on the vector of kinematic joint angles, $\boldsymbol{q}$. From this end-effector, the target marker position $\boldsymbol{t_i}$ is subtracted to find the positional error. Within this MOO approach, each distance objective is the square of the distance between the end-effector and the target marker position, normalized by the working maximum distance $\boldsymbol{d_{max}}$. Note that $\boldsymbol{w_i}$ has a value between 0 and 1 and refers to a weight corresponding to each end-effector, as defined in the protocol—these weights ensure that markers with a critical role in a motion are evaluated as such (Eq. 2.4).

2.4 Prediction of Virtual Model Anthropometry

The quality of motion capture processing relies on anthropometric measurements of the original subject. However, body dimensions are either not provided with the motion capture data or are not sufficiently accurate. When the virtual model and human subject are of significantly different sizes, the original posture cannot be effectively replicated.

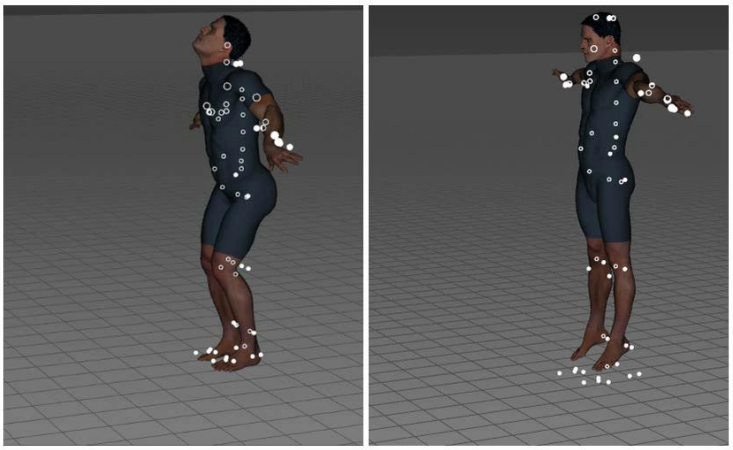

(a) (b)

Fig. 4. Effects of anthropometric differences between human model and virtual model on motion capture processing: (a) subject is much shorter than virtual model, (b) subject is much taller than virtual model.

As seen in Fig. 4, there is an adverse impact on the visualization of the motion capture data when the subject is either much taller or much shorter than the static size of the avatar. In Fig. 4a, the original human subject was much shorter than the virtual model, whereas in Fig. 4b, the original human subject was much taller than the virtual model. Both cases produce a posture that is not representative of the original motion. A technique that can successfully predict anthropometry and posture is essential in the visualization of motion capture. The initial approach to simultaneous prediction of anthropometry and posture involved optimizing the original kinematic design variables (joint angles) as well as including additional anthropometric design variables known as link-lengths.

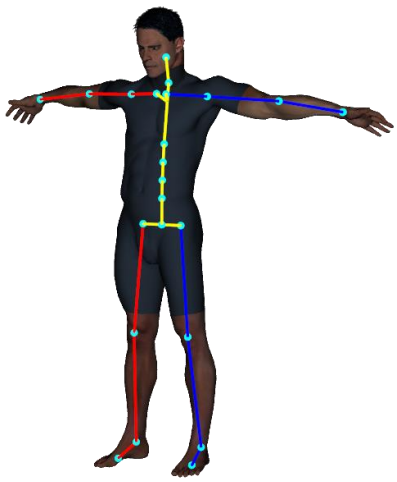

Fig. 5. Link-lengths of virtual model.

Link-lengths are the straight-line distances from one DH frame to the next that correspond to the anatomical distance between two joints, shown in Fig. 4. In posture prediction, link-lengths are traditionally given as input to the problem. However, in order to more accurately replicate the motion of subjects with body dimensions that differ from those of the virtual model, the optimization problem can be set up with the intent of finding not only kinematic joint angles, but also the anthropometric link-lengths that satisfy the given constraints and minimize the positional error between the end-effectors and the target markers.

The modified optimization problem can be presented using the following formulation:

$$
\begin{aligned}
&\boldsymbol{Find\ q\ \in\ R^{DOF}\ by\ minimizing\ the\ distance\ objectives}:\\
&\quad a.\quad f(\boldsymbol{x}(\boldsymbol{q}))\\
&Subject\ to:\\
&\quad b.\quad {q_i}^L \le\ q_i\ \le\ {q_i}^H;\ i = 1, 2, \dots, DOF\\
&\quad c.\quad {l_j}^L \le\ l_j\ \le\ {j_j}^H;\ j = 1, 2, \dots, LL\\
&\quad d.\quad \left|l_{k^R}\ -\ l_{k^L}\right| <\ \varepsilon;\ \{\ k^R, k^L\} \in\ LL_{sym}
\end{aligned}
\qquad \textbf{(2.5)}
$$

Similar to Eq. 2.3, $\boldsymbol{q}$ represents the vector of kinematic joint angles. The additional variable $\boldsymbol{l}$ represents the vector of anthropometric link-lengths that will be determined in conjunction with the joint angles. Supplementary constraints ensure that the optimal solution remains within the boundary of feasible body dimensions. Eq. 2.5c imposes limits on the anthropometric variability such that $\boldsymbol{l_j^L \le l_j \le l_j^U}$, where $\boldsymbol{l_j}$ represents the $\boldsymbol{j^{th}}$ link-length, $\boldsymbol{l_j^L}$ is its lower limit, and $\boldsymbol{l_j^U}$ is its upper limit. Additionally, Eq. 2.5d ensures that the right and left sides of the body remain symmetric, where $\boldsymbol{l_{k^R}}$ and $\boldsymbol{l_{k^L}}$ are corresponding link-lengths on the left and right sides of the body, respectively. The set of symmetric link-lengths, denoted as $\boldsymbol{LL_{sym}}$, includes the elbow-wrist, shoulder-elbow, clavicle-shoulder, sacrum-hip, hip-knee, knee-ankle, and ankle-toe distances. Using MOO, the combined objective function is defined as:

$$
\boldsymbol{f(x(q,l)) = \left[\sum_{i=1}^{n}\left(w_i \frac{\|x_i(q,l) - t_i\|^2}{d_{max}}\right)^p\right]^{\frac{1}{p}}} \qquad \textbf{(2.6)}
$$

Note that Eq. 2.6 is similar to Eq. 2.5, except that the end-effector position $\boldsymbol{x_i(q,l)}$ is now a function of both kinematic joint angles ($\boldsymbol{q}$) and anthropometric link-lengths ($\boldsymbol{l}$).

Initial implementation of link-lengths as design variables using the formulation of Eq. 2.5 did not successfully predict anthropometry, as the position of the end-effectors did not scale with the size of the virtual model during the optimization process. This caused the end-effectors to become unrealistically far from anthropometric landmarks, leading to a problem in which differences in anthropometry between the human subject and virtual model caused a distorted visualization.

3 METHODS

To improve implementation of link-lengths as design variables, it was necessary to construct end-effectors that scale to the anthropometric landmarks as link-lengths are scaled during the optimization process. In Eq. 3.1, the end-effectors are represented with local positions rigidly attached to the parented joint, using the standard DH transformation [11]:

$$\boldsymbol{x_i}(\boldsymbol{q}, \boldsymbol{l}) = \left(\prod_{j=1}^{n} {}^{j-1}\boldsymbol{T}_j(\boldsymbol{q}, \boldsymbol{l}) \right) \boldsymbol{x}_i^{local} \tag{3.1}$$

The position of the virtual model can be determined by successive multiplication of transformations [5]. The local position, denoted as $\boldsymbol{x}_i^{local}$, refers to the position of the end-effector on the virtual model, which is defined in the mapping protocol as a fixed value and is thus unaffected by the link-length design variables (Eq. 3.1).

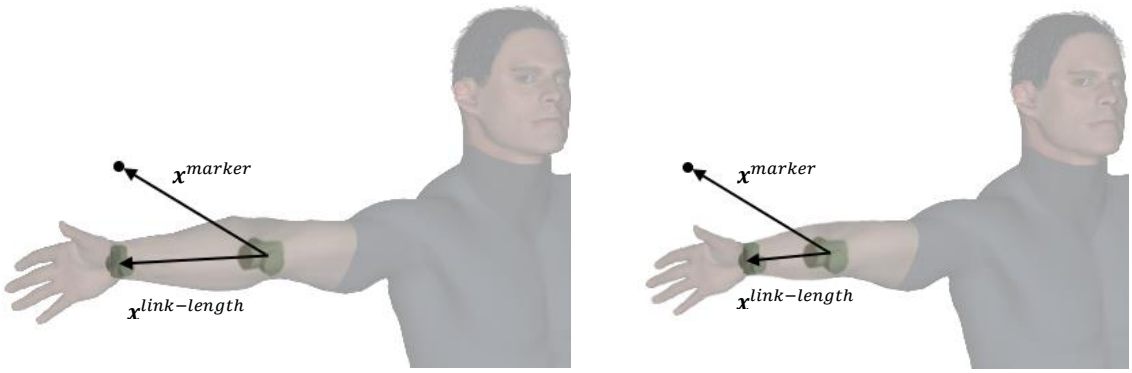

(a) (b)

Fig. 6. Fixed marker position (a) before and (b) after modifying link-length.

In Fig. 6. Fixed marker position (a) before and (b) after modifying link-length.

a and Fig. 6. Fixed marker position (a) before and (b) after modifying link-length.

b, the position of the marker ($\boldsymbol{x}^{marker}$) represents the same anatomical landmark on the forearm. Fig. 6. Fixed marker position (a) before and (b) after modifying link-length.

a displays the position of the marker prior to running posture prediction using link-lengths as design variables. When a link-length is modified, represented in Fig. 6. Fixed marker position (a) before and (b) after modifying link-length.

b, the end-effector no longer represents the same anatomical position, since the coordinates of $\boldsymbol{x}^{marker}$ have not changed.

A new method was developed using flexible marker positions, which represent end-effectors relative to the link-lengths. Using flexible marker positions, the end-effector moves proportionally as anthropometric measurements are modified, so that it stays relative to the same anatomical landmark, as shown in Fig. 7. Flexible marker position (a) before and (b) after modifying link-length.

. The flexible marker position is implemented by describing the marker position ($\mathbf{x}^{\text{marker}}$) relative to both of the link-length endpoints, rather than fixed to a parent joint.

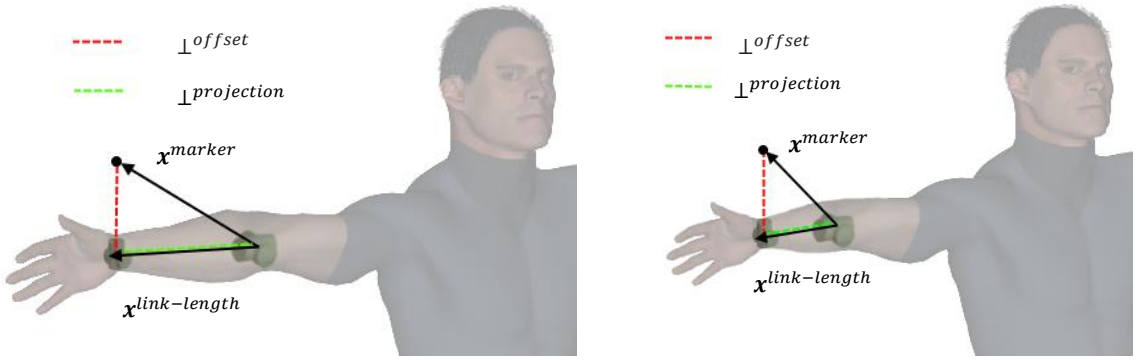

(a) (b)

Fig. 7. Flexible marker position (a) before and (b) after modifying link-length.

First, $\boldsymbol{x}^{marker}$ is projected onto the centerline of the corresponding link-length, $\boldsymbol{x}^{link-length}$, as shown in Fig. 7. Flexible marker position (a) before and (b) after modifying link-length.
by the dashed yellow line long the limb, using Eq. 3.2.

$$\perp^{projection} = \left| \frac{\boldsymbol{x}^{marker} \bullet \boldsymbol{x}^{link-length}}{\boldsymbol{x}^{link-length} \bullet \boldsymbol{x}^{link-length}} \right| \quad \textbf{(3.2)}$$

Next, the position of the marker along the centerline of the link-length is described using a percentage of its distance between the endpoints of the link-length, $\%^{link-length}$, as shown in Eq. 3.3.

$$\%^{link-length} = \left| \frac{\perp^{projection}}{\boldsymbol{x}^{link-length}} \right| \quad \textbf{(3.3)}$$

The marker is translated from its position along the centerline of the link-length to the skin of the virtual model using an offset vector, $\perp^{offset}$, which is represented by the dashed red line in Fig. 6 (Eq. 3.4).

$$\perp^{offset} = \boldsymbol{x}^{marker} - \perp^{projection} \quad \textbf{(3.4)}$$

The result of Eq. 3.2 represents the position of the end-effector, were it to be directly placed on the centerline of the body segment, as a percentage of the total segment length. Because this percentage remains constant throughout the optimization process, it can be used to describe the proportional

distance of the end-effector along the centerline as the link-lengths are modified by multiplying the percentage and the link-length vector. Then, the flexible position $\boldsymbol{x_i}^{\boldsymbol{local}}(\boldsymbol{l})$ is defined in Eq. 3.5 and takes the place of the fixed position in the distance objective in Eq. 3.1. Thus, as the link-lengths change, the position of the marker will change proportionally, allowing it to represent more accurately the appropriate anatomical position.

$$\boldsymbol{x}_i{}^{local}(l) = \%^{link-length} \cdot (\boldsymbol{x}^{next} - \boldsymbol{x}^{parent}) + \perp^{offset} \tag{3.5}$$

$$\boldsymbol{x_i}(\boldsymbol{q}, \boldsymbol{l}) = \left(\prod_{\boldsymbol{j=1}}^{\boldsymbol{n}} {}^{j-1}\boldsymbol{T}_j(\boldsymbol{q}, \boldsymbol{l}) \right) \boldsymbol{x_i}{}^{local}(\boldsymbol{l}) \tag{3.6}$$

Note that in Eq. 3.5, the vector from the parent joint center $\boldsymbol{x}^{parent}$ to the next joint center $\boldsymbol{x}^{next}$ is dependent on the current values of the link-length design variables**.**

4 RESULTS

4.1 Motion Capture Data

In order to test the prediction of anthropometry using the new, flexible end-effector, Motion capture data was used from variable subjects performing similar tasks. Three male subjects performed a walking motion consisting of four 180-degree turns, such that the subject was walking in either the left or right direction relative to the viewport. From each motion, five key frames were selected for analysis. These key frames were selected based on the representative points of a single gait cycle while running. Specifically, these phases are described by Novacheck [15] as stance phase absorption, stance phase generation, swing phase generation, swing phase reversal, and swing phase absorption. Note that swing phase reversal was not used as a key frame in this paper; also, an additional neutral posture frame was included, during which the subject was instructed to stand in a comfortable position prior to any movement. In addition to these key frames, the anthropometric dimensions of each subject were compared over the entire motion.

Prior to capturing the motion, body dimensions were measured in accordance with the MVN User Manual, developed by Xsens Technologies B.V. [16]. These measurements were later compared to the body segment dimensions of the virtual model to evaluate the accuracy of the predicted link-lengths. The varying anthropometric dimensions of each subject, along with the default dimensions of the virtual model, are presented in Table 1.

Table 1. Anthropometric dimensions of subjects and default dimensions of virtual model.

Dimension (cm)	Subject 1	Subject 2	Subject 3	Model
Body Height	166.0	174.0	193.0	182.0
Hip Height	85.0	91.5	100.0	84.5
Knee Height	48.9	51.0	60.0	53.3

Arm Span	162.0	175.0	192.4	196.2
Hip Width	27.5	25.0	28.0	28.4
Shoulder Width	37.4	35.0	42.0	37.7

Corresponding body segments of the virtual model were determined after optimization at each frame through the addition of link-lengths representing one of the above dimensions. However, the head and hands are not represented by link lengths; therefore, their anthropometry is not optimized, meaning their size is also equal across the various subjects' motions. To determine body height and arm span, the fixed values of the head and hands were added to the length of each corresponding segment. Additionally, because the body segments of the virtual model only represent the distance between internal joint center locations, offsets were implemented to account for the length between the joint and the anatomical landmark at which the measurement was taken on the original subjects.

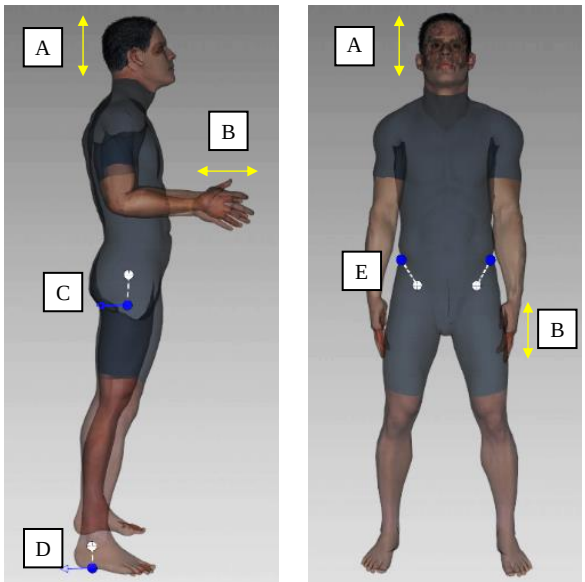

Fig. 8. Fixed offsets representing length of (A) head, (B) hand, (C) hip joint center to greater trochanter, (D) ankle joint center to floor, and (E) hip joint center to anterior superior iliac spine.

In Fig. 8, the head and hands offset are illustrated on the virtual model at points A and B, respectively. Additionally, because the body segments of the virtual model only represent the distance between internal joint center locations, offsets were used to account for the distance between the joint center and the appropriate anatomical landmark at which the measurement was taken on the human subjects. Each of these offsets is displayed on the model. The body height, hip height, and knee height are increased by the distance from the floor to the ankle joint center (D). Additionally, the hip height was decreased by the vertical distance from the hip joint center to the superficial prominence of the greater trochanter (C), and the hip width was increased by the horizontal distance from the left and right hip joint center to the anterior superior iliac spine (E).

4.2 Link-Lengths as Design Variables

Incorporating link-lengths as design variables using fixed marker positions yielded improved predicted postures in limited cases. However, in many cases, the resulting postures and anthropometries were unrealistic, due to the inaccuracies of fixed marker positions used to minimize the position error. Using the flexible marker positions visually improved the predicted postures and consistently resulted in predictions that are more accurate, as displayed in Fig. 9.

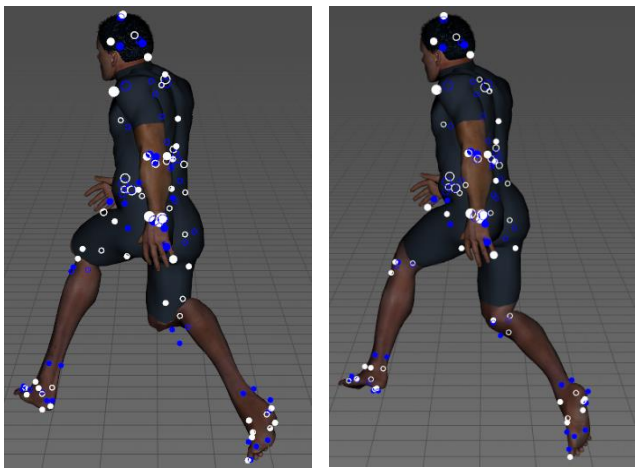

(a) (b)

Fig. 9. Result of running posture prediction on a single frame of Motion capture data (a) with anthropometric design variables using fixed marker positions, and (b) with anthropometric design variables using flexible marker positions.

Markers associated with the motion capture data (targets markers) are depicted in blue, while the corresponding end-effectors are depicted in white. The motion data is of Subject 1, who is much smaller relative to the default measurements of the virtual model (Fig. 9). Specific anthropometric measurements are documented in Table 1. Fig. 9a depicts the use of fixed end-effectors during prediction of both posture and anthropometry. To minimize the positional error between the virtual and target markers, the link-lengths of the virtual model should have decreased. However, the end-effectors were fixed, causing misrepresentation of the anatomical landmark. As a result, posture prediction produced a solution in which the knee is bent at an unrealistic angle in order to minimize the distance between then virtual and target markers. This unrealistic angle is also in part due to the skinning of the high-fidelity model, which emphasizes discrepancies between the virtual and Target markers.

Comparison of the same frame in the motion data of Subject 1 highlights the improvements observed across all of the frames and subjects when using flexible marker positions. The flexible representation allowed the relative position of the end-effector to scale proportionally as link-lengths were modified. Thus, the end-effectors stayed near their associated anthropometric landmarks throughout the optimization process (Fig. 9b). As such, the predicted posture was visually more plausible, which is particularly evident at the knee.

4.3 Comparison of Anthropometry Prediction using Fixed and Flexible End-Effectors

Depicting the same frame using both the fixed and flexible end-effector positions provides a qualitative basis of support for the flexible method, which produced a visually more realistic posture. Deeper analysis using quantitative comparison of the body dimensions of the virtual model and original subject also indicates that the flexible method results in predicted anthropometry closer to that of the original subject.

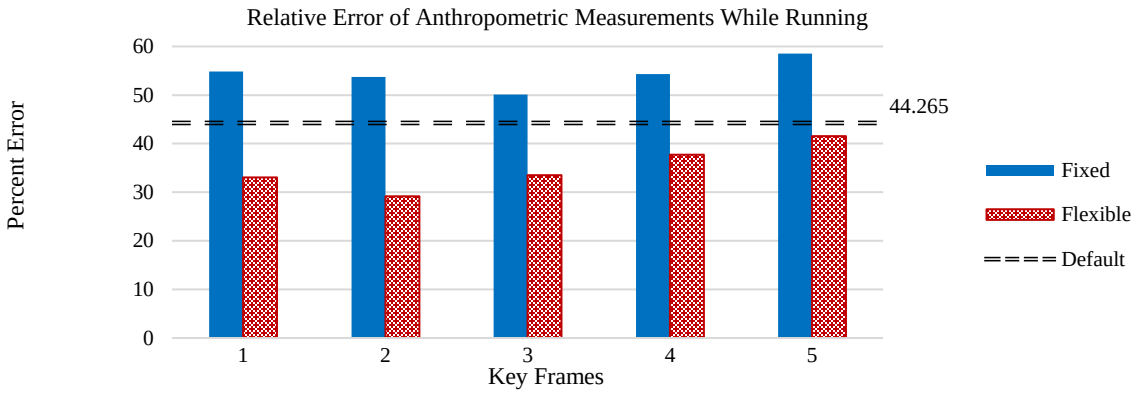

Fig. 10. Relative error in predicted anthropometry at five key frames (Section 4.1) averaged over subjects.

Using the five key frames described in Section 4.1, percentage error in body dimension was calculated using the original subject's measurements as the expected values and the virtual model's predicted measurements as the experimental values. The results in Fig. 10 are the sum of the percentage error at each body dimension, averaged across the three subjects. The default line corresponds to the absolute error in the virtual model's default body dimensions. That is, it represents the error in body dimension when no anthropometric design variables are predicted. At the five frames selected, optimization using the flexible marker positions resulted in anthropometric measurements with a lower percentage of error across all of the subjects (Fig. 10).

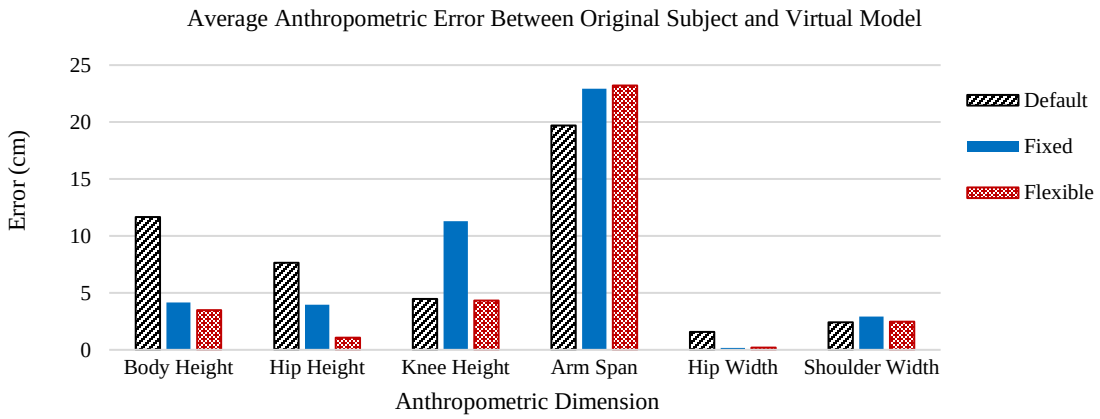

Fig. 11. Average of the absolute errors of each predicted body dimension calculated every 5-10 frames of motion.

The absolute error was calculated every five to ten frames over the entire motion and averaged across these frames. This process was repeated for all three subjects, and the average across the subjects is illustrated in Fig. 11. Visualization of the absolute error in the predicted anthropometry of the virtual model with regard to that of the original subject suggests on a quantitative basis that the use of flexible marker positions during Motion capture processing decreases the error between the anthropometry of the original subject and the virtual model. Note that there is a large amount of error associated with the arm span dimension in all cases. This is in part because the body dimensions of the original subjects were measured while the subjects stood in a T-pose, as shown in

Most motion capture systems provide the three-dimensional Cartesian position of each target marker placed on the subject at each frame of the motion, allowing the positions of the target markers to be represented in a virtual environment at each frame [12]. For the purposes of this paper, processing such motion capture data refers to using these target marker positions as input to replicate the motion on a virtual model, where the motion is ultimately described by a vector of joint angles that changes over time. Markers of this type will be referred to as target markers, as they are the end positional target of a corresponding end-effector.

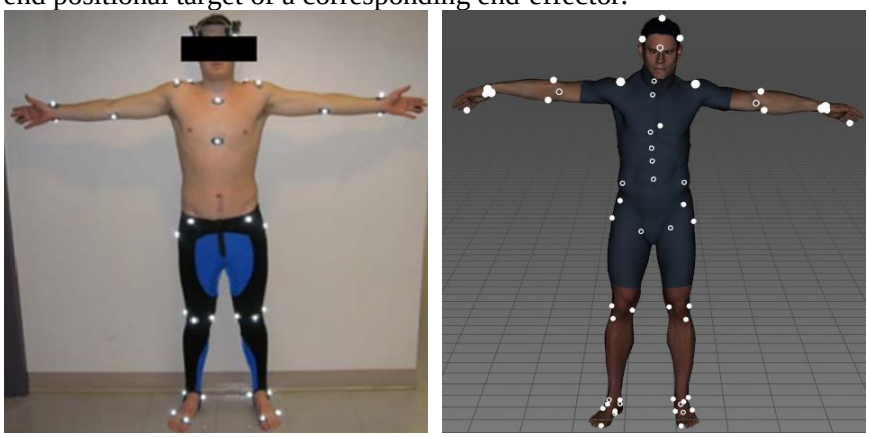

(a) (b)

Fig. 2. Mapping Target markers on the human subject onto the virtual model: (a) target markers [13] (b) virtual end-effectors.

A mapping protocol is used to place end-effectors on the virtual model (**Error! Not a valid bookmark self-reference.**b), which correspond to the anatomical locations of the target markers as they were placed on the subject (**Error! Not a valid bookmark self-reference.**a). The protocol defines each of these end-effectors relative to a parent joint on the high-fidelity human model and maps each marker onto the model relative to a global coordinate system in three-dimensional space [13].

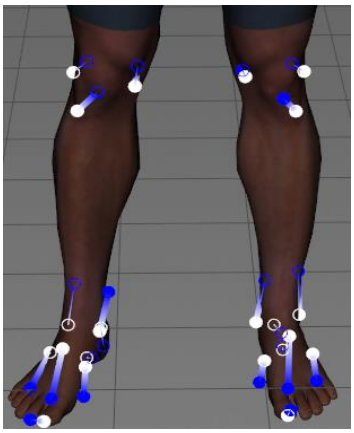

Fig. 3. Close-up of distances between target markers (white) and end-effectors (blue) on virtual model.

In Fig. 3, the end-effectors are depicted in blue. To process an individual frame of the motion capture data, a distance objective is created for each end-effector to minimize the distance to its mapped target obtained from the motion capture data. To replicate an entire motion, posture prediction is executed over all frames to determine joint angles using the formulation defined in Eq. 2.3.

. In the motion analyzed for this work, the arms of the subject remained close to the body for most frames, and this affected the predicted arm span.

5 DISCUSSION

5.1 Significance

The overall quality of the motion capture processing and resulting visualization are dependent on the presence and accuracy of the anthropometric measurements, which are highly variable. This paper proposes a method that integrates the functionality of an anthropometric model and biomechanical model into a single entity, thus allowing for simultaneous prediction of anthropometry and posture using optimization-based techniques. Ultimately, this increases the accuracy of the visualization of the motion capture data on the virtual model. When quantitatively compared to methods that either lack anthropometry prediction or possess anthropometry prediction that does not use the flexible end-effector, the new, flexible method for anthropometry prediction clearly depicted more success.

Because biomechanical studies often rely on a mathematical description of motion to provide a basis for quantitative evaluation of human performance, the accuracy of motion capture processing is critical. Overall, the results provided in this paper indicate that simultaneous prediction of anthropometry and posture is a feasible method of improving motion capture processing and visualization.

5.2 Limitations

As in any research endeavor, features not considered in this particular approach leave room for future development. The first of these is the implementation of modifiable link-lengths for the head and hands. Quite obviously, the anthropometry of these body segments is not equivalent across the population. Incorporating them in the optimization process is essential in producing the most accurate motion possible, though the results achieved in using the current approach discussed in this paper were highly realistic. Additionally, the approach discussed in this paper aims only to produce segment lengths closer to that of the original subject; it does not estimate the thickness of these segments to any extent. If the body type of the subject is different from the virtual model on which the motion capture data is processed, the results will be less accurate. Link-length modification tends to overcompensate, as it tries to accommodate for lengthwise and radial differences by altering only length. Furthermore, the processing the motion of two equal-height subjects with highly differentiable weight or muscle tone should result in a virtual model with a similar body shape; however, the model would only have similar body segment lengths. The actual shape of the model may be either thicker or thinner than the original subject.

The effectiveness of the new, flexible end-effector was validated using the average anthropometric error between the measurements of the original human subject and the virtual model after optimization-based posture prediction. However, the method should be further validated through comparison of the actual, individual marker locations on the original subject to the end-effectors on the avatar. Furthermore, to produce more accurate data, this comparison should be done with the subject and virtual model in the same pose. Additional validation should also focus on the accuracy in the biomechanical analysis by recording biomechanical factors on the original subject.

5.3 Future Work

The current approach only considers the lengthwise dimensions; thus, integrating the thickness of each segment should be investigated to further improve the accuracy of biomechanical analysis. In addition to joint angle and link-length, an offset could be included as a design variable, thus integrating the thickness of the segment into the optimization formulation to further improve the current implementation.

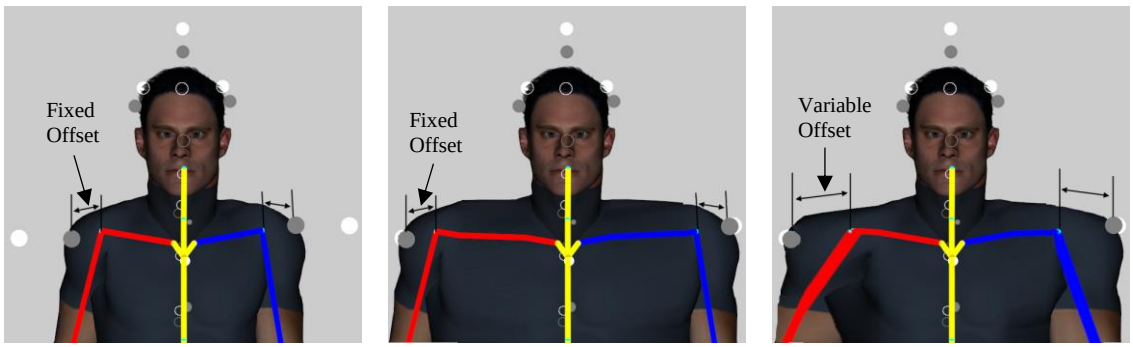

Fig. 12 Theoretical effects of fixed offset versus variable offset in prediction of anthropometry.

Ideally, the inclusion of design variables that represent segment thickness would produce the results depicted in Fig. 12. In the optimal case, the thickness of the segment would increase, allowing posture prediction to minimize the distance between a target and end-effector using kinematic joint angles, link-lengths, and link thickness offsets to best replicate body dimensions and posture.

6 CONCLUSION

In this paper, a new approach to improve motion capture processing using virtual models was presented. This approach incorporated both anthropometric and kinematic design variables to minimize the distance between Target markers and the corresponding end-effectors on the virtual model. This optimization-based approach produced realistic motion with anthropometric measurements close to those of the original subject and improved the overall appearance of the virtual model. Because the anthropometry of the virtual model more closely replicates that of the original subject, the solution provides the means for more accurate biomechanical analysis. Nonetheless, the use of flexible marker positions provides an effective framework for more accurate processing of Motion capture data without the need for pre/post-processing, which can be extended to further improve the reliability of biomechanical analysis of the processed motion.

ACKNOWLEDGEMENTS

This work is funded by the US Office of Naval Research, under program W911QY-12-C-0009. Specific thanks to Kimberly Farrell, Ross Johnson, Timothy Marler, Salam Rahmatalla, Rajan Bhatt, and Karim Abdel-Malek for their prior contributions to the project, and additional thanks to all others on the team at the University of Iowa's Virtual Soldier Research program, whose continuous developments have made this research possible.

REFERENCES

[1] Xiang, Y., Rahmatalla, S., Arora, J., Abdel-Malek, K: Enhanced optimization based inverse kinematics methodology considering joint discomfort. In: Int. J. Human Factors Modelling and Simulation, vol. 2, nos 1/2, pp. 111--126 (2011)

[2] Bonin, D., Wischniewski, S., Wirsching, H.-J., Upmann, A., Rausch, J., Paul, G.: Exchanging data between Virtual Modelling systems: a review of data formats. In: 3rd International Virtual Modeling Symposium, Odaiba, Tokyo, Japan (2014)

[3] Li, P., Carson, J., Parham, J., Paquette, S.: Virtual Modeling Pipeline with 3D Anthropometry Database. In: Duffy V. (eds) Advances in Applied Virtual Modeling and Simulation, vol 481. Springer, Cham, Switzerland. (2017)

[4] Yang, J., Rahmatalla, S., Marler, T., Abdel-Malek,K., Harrison, C.: Validation of predicted posture for the virtual model Santos®. In: Duffy V. (eds) Virtual Modeling, 4561, pp. 500—510. Springer, Cham, Switzerland. (2007)

[5] Denavit, J., Hartenberg, R.S.: A kinematic notation for lower-pair mechanisms based on matrices. In: Journal of Applied Mechanics, vol. 77, pp. 215--221 (1955)

[6] Farrell, K., Marler, R. T., Abdel-Malek, K.: Modeling Duel-Arm Coordination for Posture: An Optimization-Based Approach. In: SAE Technical Paper number 2005-01-2686, Virtual Modeling for Design and Engineering Symposium, Iowa City, Iowa (2005)

[7] Marler, R. T.: A Study of Multi-Objective Optimization Methods for Engineering Applications. VDM Verlag, Saarbrucken, Germany (2009)

[8] Marler, R. T., Arora, J. S., Yang, J., Kim, H. –J., and Abdel-Malek, K.: Use of Multi-objective Optimization for Virtual model Posture Prediction. In: *Engineering Optimization*, vol. 41 pp. 295--943 (2009)

[9] Marler, R. T., Rahmatalla, S., Shanahan, M., Abdel-Malek, K.: A New Discomfort Function for Optimization-Based Posture Prediction. In: SAE Technical Paper number 2005-01-2680, Virtual modeling for Design and Engineering Symposium, Iowa City, Iowa (2005)

[10] Marler, R. T., Farrell, K., Kim, J., Rahmatalla, S., and Abdel-Malek, K.: Vision Performance Measures for Optimization-Based Posture Prediction. In: SAE Technical Paper number 2006-01-2334, Virtual Modeling for Design and Engineering Conference, Lyon, France (2006)

[11] Abdel-Malek, K., Arora, J.: Human motion simulation: predictive dynamics. In: Academic Press (2013) doi: 10.1016/B978-0-12-405190-4.00011-8

[12] Motion Lab Systems, Inc.: The C3D File Format: User Guide. LA: Author (2008). Retrieved from https://www.projects.science.uu.nl/umpm/c3dformat_ug.pdf.

[13] Rahmatalla, S., Xiang, Y., Smith, R., Li, J., Muesch, J., Bhatt, R., Swan, C., Arora, J., Abdel-Malek, K,: A Validation Protocol for Predictive Human Locomotion. In: SAE Technical Paper number 2008-01-1855, Virtual Modeling for Design and Engineering Conference, Pittsburgh, PA (2008)

[14] Marler, R. T., Arora, J.: Survey of multi-objective optimization methods for engineering. In: Structural and Multidisciplinary Optimization, vol. 26, pp. 369—395. Springer, Cham, Switzerland. (2004)

[15] Novacheck, T.F.: The biomechanics of running. In: Gait and Posture, vol. 7 pp.77--95. Elsevier (1998)

[16] XSens Technologies B.V.: MVN Motion Capture System: User Manual. CA: Author (2013) Retrieved from https://www.xsens.com/xsens-mvn-documentation.

[17] Seydel A. et al. (2018) Improved Motion Capture Processing for High-Fidelity Human Models Using Optimization-Based Prediction of Posture and Anthropometry. In: Cassenti D. (eds) Applied Human Factors and Ergonomics: Advances in Human Factors in Simulation and Modeling. Advances in Intelligent Systems and Computing, vol 591. Springer, Cham, Switzerland. (2017).